Available online at www.sciencedirect.com
ScienceDirect
Journal of Catalysis 246 (2007) 136–146
JOURNAL OF CATALYSIS
www.elsevier.com/locate/jcat

# *Gem*-diamines as highly active organocatalysts for carbon–carbon bond formation

María J. Climent, Avelino Corma *, Irene Domínguez, Sara Iborra, María J. Sabater, Germán Sastre

*Instituto de Tecnología Química UPV-CSIC, Av. Los Naranjos, s/n 46022, Valencia, Spain*

Received 28 September 2006; revised 28 November 2006; accepted 28 November 2006

Available online 4 January 2007

**Abstract**

Diamines with neighbour nitrogen atoms have been used as base catalysts in the Knoevenagel condensation reaction between benzaldehyde and ethyl cyanoacetoacetate. The catalytic results show that a good basic catalyst requires a combination of two factors: high proton affinity and the ability to return the proton to the oxoanion intermediate. Computational chemistry calculations show this by characterizing the reactants, products, and transition states and by calculating the activation energies of the different reaction steps. A diamine, di(3-methylpiperidine)methane (**B**), has been found with a higher catalytic activity than **DMAN** despite its lower proton affinity, demonstrating that not only the proton affinity, but also the steric ability to abstract the protons, are important in explaining the catalytic results.
© 2006 Elsevier Inc. All rights reserved.

*Keywords:* *Gem*-diamines; Basic catalysis; Computational chemistry; Knoevanagel condensation

## 1. Introduction

The development of clean processes for production of fine chemicals has driven research in the areas of solid base- and organic base-supported catalysts [1]. Micelle template silicas (MTS), such as MCM-41, containing a large number of silanol groups that allows the grafting of amines, provide an excellent inorganic support for producing heterogenized base catalysts with tailored pore sizes and high surface areas, in which the basicity can be controlled by changing the p$K_a$ of the grafted amine. Primary, secondary, and tertiary amines [2] ammonium hydroxide [3], guanidines [4], diamines, and proton sponges [5] have been grafted on MTS and used as heterogeneous basic catalysts for various basic catalyzed organic reactions, such as aldol and Knoevenagel condensations, alkylation and elimination reactions, Michael-type additions, transesterifications, and so on [6]. Among these, diamines with neighbouring nitrogen atoms at short distances and aromatic frames, such as naphthalene, fluorine, and phenantrene, which are denominated proton sponges, show a well-defined and strong basicity [7]; for instance, the proton sponge 1,8-bis(dimethyl amino) naphthalene (**DMAN**; see Scheme 1) has a p$K_a$ of 12.1. It has been proposed that the steric strain is the main reason for the high basicity constant of these compounds [8]. Thus, it has been reported that **DMAN** or **DMAN** supported on MCM-41 is an excellent base catalyst for Knoevenagel and Claisen–Schmidt condensations [5,9].

Knoevenagel condensation is widely used in organic synthesis to produce important intermediates and end products for perfumes, pharmaceuticals, and polymers [10] (Scheme 1). It can be catalyzed by a wide variety of bases from weak to strong basicities and has proven to be a very adequate test reaction for base catalysis. In fact, reacting benzaldehyde with compounds containing activated methylenic groups with different p$K_a$ values, such as ethyl cyanoacetate (p$K_a \leqslant 9$), ethyl acetoacetate (p$K_a \leqslant 10.7$), and diethyl malonate (p$K_a \leqslant 13.3$), makes it possible to evaluate the basic strength of a catalyst [11]. The kinetics of the Knoevenagel reaction have been widely studied, and it is generally agreed [12] that the reaction is first order with respect to each reactant and the catalyst.

In the present work, different diamines with vicinal nitrogen atoms that exhibit a strong basic character have been prepared. The behaviour of these stable diamines as homogeneous base catalysts for the Knoevenagel condensation reaction of ben-

* Corresponding author.
*E-mail address:* acorma@itq.upv.es (A. Corma).

0021-9517/$ – see front matter © 2006 Elsevier Inc. All rights reserved.
doi:10.1016/j.jcat.2006.11.029

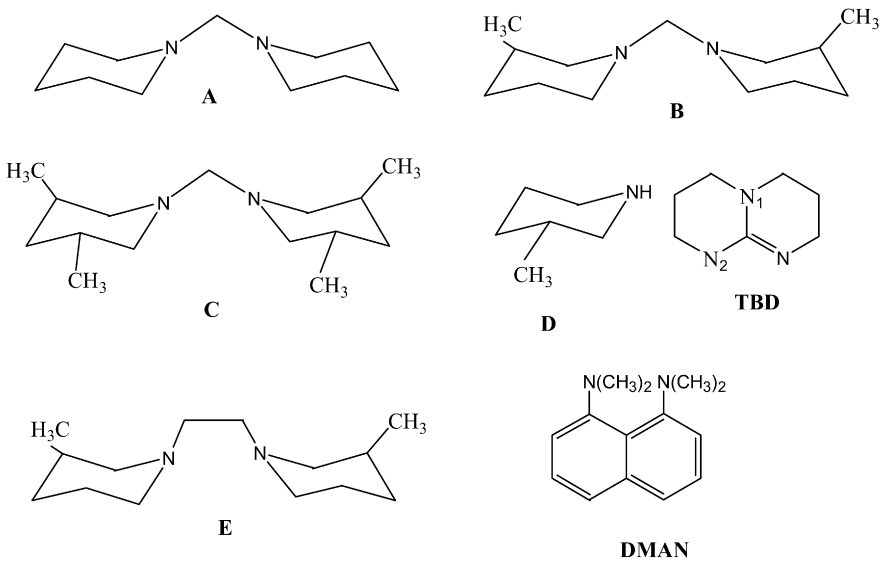


Scheme 1. Schematic representation of dipiperidinemethane (amine **A**), di(3-methylpiperidine)methane (amine **B**), di(3,5-dimethylpiperidine)methane (amine **C**), 3-methylpiperidine (amine **D**), 1,5,7-triazabicyclo[4.4.0]dec-5-ene (**TBD**) and 1,8-bis(dimethyl amino) naphthalene (**DMAN**).

zaldehyde with reactants with different p$K_a$ values has been studied. To explain the catalytic results, the proton affinities of the different amines have been calculated and the interactions between the transition state complexes and the base catalyst established. This work demonstrates that these *gem*-diamines behave as strong homogeneous base catalysts and are excellent candidates for heterogenization.

## 2. Experimental

### 2.1. Synthesis of the amines

Amines **A** and **B** are known compounds and were prepared according to a procedure described in the patent literature [13].

#### 2.1.1. Synthesis of dipiperidinemethane (*A*)

A 50-mL round-bottomed flask was charged with 3.74 g (44 mmol) of piperidine, 0.66 g (22 mmol) of paraformaldehyde, and 17 mL of acetonitrile. The mixture was heated to reflux for 20 h. The solvent was evaporated to dryness, and the residue was distilled under vacuum to give 3.1 g of the diamine **A** (yield: 78%). Spectroscopic data were as follows: $^1$H NMR (300 MHz, $CDCl_3$): $\delta = 1.42$–$1.44$ (m), 1.51–1.56 (m), 2.38–2.40 (m) and 2.82 (s) ppm; $^{13}$C NMR (75 MHz, $CDCl_3$): $\delta = 25.3$, 26.5, 53.4 and 83.1 ppm; IE-MS ($m/z$): 182 ($M^+$), 110, 97, 84.

#### 2.1.2. Synthesis of di(3-methylpiperidine)methane (*B*)

A 50-mL round-bottomed flask was charged with 4.35 g (44 mmol) of 3-methylpiperidine, 0.66 g (22 mmol) of paraformaldehyde, and 17 mL of acetonitrile. The mixture was heated to reflux for 20 h. The solvent was evaporated to dryness, and the residue was distilled under vacuum to give 4.1 g of the diamine **B** (yield: 90%). Spectroscopic data were as follows: $^1$H NMR (300 MHz, $CDCl_3$): $\delta = 0.9$ (d), 1.4–1.8 (m), 1.8 (t), 2.8 (s) ppm; $^{13}$C NMR (75 MHz, $CDCl_3$): $\delta = 20.1$, 25.9, 31.4, 33.9, 53.0, 60.9 and 82.7 ppm; IE MS ($m/z$): 209 ($M^+$), 112, 98.

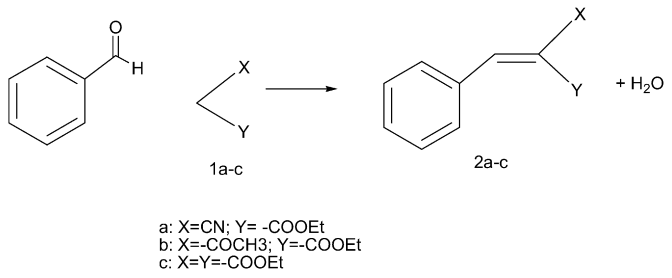


Scheme 2. Schematic representation of the Knoevenagel condensation between benzaldehyde and carboxylates **1a**–**1c**.

#### 2.1.3. Synthesis of di(3,5-dimethylpiperidine)methane (*C*)

The same procedure was applied for the synthesis of amine **C**. A 50-mL round-bottomed flask was charged with 4.97 g (44 mmol) of 3,5-dimethylpiperidine, 0.66 g (22 mmol) of paraformaldehyde, and 17 mL of acetonitrile. The mixture was heated to reflux for 20 h. The solvent was evaporated to dryness, and the residue was distilled under vacuum to give 4.6 g of the diamine (yield: 89%). Spectroscopic data were as follows: $^1$H NMR (300 MHz, $CDCl_3$): $\delta = 0.9$ (d), 1 (d), 1.4 (t) and 2.9 (s) ppm; $^{13}$C NMR (300 MHz, $CDCl_3$): $\delta = 19.7$, 31.0, 42.9, 59.9 and 82 ppm; IE-MS ($m/z$): 238 ($M^+$), 237, 126, 112, 110, 98, 97, 83, 84. Elemental analysis: found—75.3% C, 12.7% H, 11.7% N; $C_{15}H_{30}N_2$; requires—75.6% C, 12.6% H, 11.8% N.

#### 2.1.4. Synthesis of 1,2-di(3-methylpiperidine)ethane (*E*)

A 100-mL round-bottomed flask was charged with 3.1 g (31.3 mmol) of 3-methylpiperidine, 13.3 g (96.2 mmol) of $K_2CO_3$, and 40 mL of chloroform. The mixture was stirred at room temperature for 15 min, and 1.4 mL (16.4 mmol)

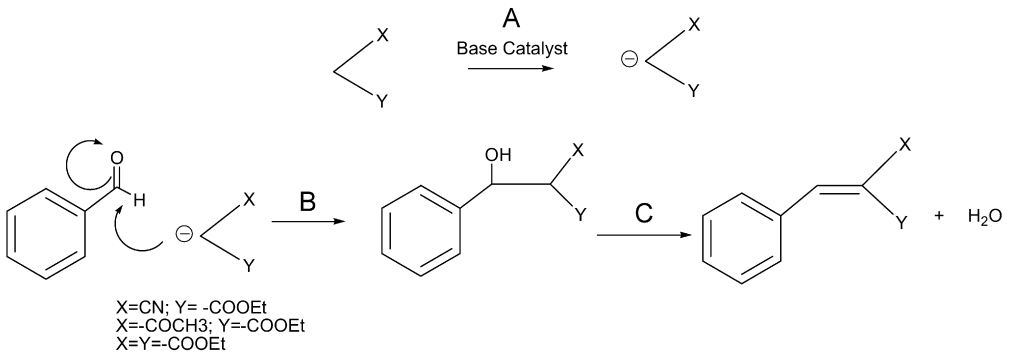


Scheme 3. Mechanism of the Knoevenagel condensation reaction. (A) Formation of the carbanion on the methylenic group upon the action of the basic catalyst; (B) attack of this carbanion intermediate to the carbonyl group and (C) elimination of the hydroxyl group to form a C=C bond and water.

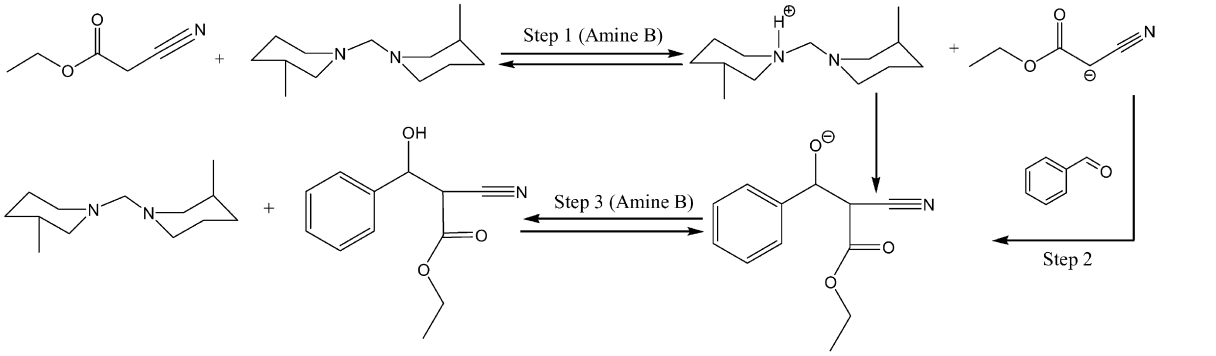


(1)

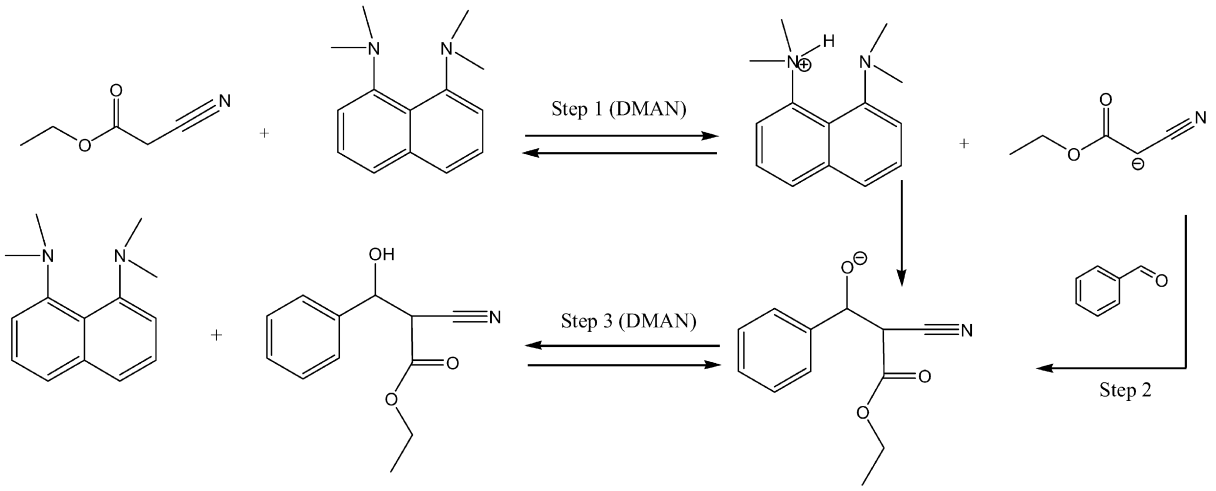


(2)

Scheme 4. Reaction steps that take place in the condensation between the ethyl cyanoacetate and benzaldehyde using amine **B** (reaction (1)) and using **DMAN** (reaction (2)) as catalyst. Step 1 is the proton transfer from the ethyl cyanoacetate to the catalyst; step 2 is the formation of the oxoanion intermediate; and step 3 is the release of the proton from the catalyst to the oxoanion to give the Knoevenagel condensation product.

of 1,2-dibromoethane was added. The suspension was stirred at room temperature while being monitored by chromatography. The solid was filtered off and washed with chloroform. The organic extracts were dried with $Na_2SO_4$, filtered, and concentrated to dryness to give a white solid (yield: 78%). Spectroscopic data were as follows: $^1$H NMR (300 MHz, $CDCl_3$): $\delta = 0.8$ (d), 1.5–1.7 (m), 1.8–1.9 (m), 2.4 (s) and 2.8 (t) ppm; $^{13}$C NMR (300 MHz, $CDCl_3$): $\delta = 25.6$, 31.4, 32.8, 33.0, 54.5, 56.6 and 62.6 ppm; IE-MS ($m/z$): 224 ($M^+$), 126, 112. Elemental analysis: found—74.6% C, 12.7% H, 12.3% N; $C_{14}H_{28}N_2$; requires—75% C, 12.5% H, 12.5% N.

### 2.1.5. General procedure for the Knoevenagel reactions

In a typical experiment, 0.14 mmol of the basic catalysts were added to a solvent-free solution of ethyl cyanoacetate (3.1 g, 28 mmol) while being stirred under inert atmosphere. After temperature adjustment, 0.85 g of benzaldehyde (3.4 g, 32 mmol) was added, with the reaction periodically monitored by gas chromatography using a Hewlett Packard GC 5988 A

with an FID detector and an EQUITY$^{TM}$-5 Fused silica capillary column of 5% phenylmethylsilicone. Dodecane was used as an internal standard in all of the experiments.

*2.1.6. Quantum chemical calculations*

Quantum chemical calculations were performed at the ab initio Hartree–Fock (HF) level of theory using the 3-21G basis sets [14]. We chose this method in an attempt to reach a compromise between accuracy and computational cost. This methodology was used to characterise all of the reaction intermediates in the condensation reaction of benzaldehyde and ethyl cyanoacetate, using amine **B** (see Scheme 1) as the catalyst. The global minima of the reactant and product species were optimised using Schlegel's algorithm [15], which includes the rational function optimisation (RFO) approach [16]. The transition states were fully characterised by the TS search algorithm [17], and the vibrational frequencies were subsequently calculated by determining the second derivatives of the energy with respect to the Cartesian nuclear coordinates and then transforming to mass-weighted coordinates. This allowed us to verify that only one eigenvalue was negative, corresponding to a transition state species. We did not include zero point energies and other more sophisticated techniques for characterising the energy of the reactions in our energy calculations, because we were interested only in comparing the different reaction steps as shown in Scheme 4. For the calculation of proton affinities, a density functional methodology with the B3LYP [18] functional and the 6-31G** basis set [19] was used. All quantum chemical calculations were performed using GAUSSIAN98 [20].

## 3. Results and discussion

To check the basicity of the different synthesised diamines (**A**, **B**, and **C**; Scheme 1), we used the Knoevenagel reaction as the reaction test. Thus, condensation between benzaldehyde and ethyl cyanoacetate was carried out in the absence of solvent at room temperature using the different diamines as base catalysts (Scheme 2). In all cases, the *E* and *Z* isomers of $\alpha$-ethyl-2-cyanocinnamate in an $E/Z$ ratio >160 were obtained with a selectivity of 100%.

The accepted mechanism for the base-catalyzed Knoevenagel condensation involves a first step in which the formation of the carbanion on the methylenic group occurs by abstraction of the proton by the basic catalyst. This is followed by attack of the carbanion intermediate to the carbonyl group. Finally, elimination of the hydroxyl group occurs to form a C=C bond and water, while the basic site is restored (Scheme 3).

The kinetic curves obtained with catalysts **A**, **B**, and **C** are given in Fig. 1. As shown, the conversion of ethyl cyanoacetate was 55% in the presence of diamine **A** after 30 min of reaction time. In contrast, when two methyl groups were introduced in the cyclohexane ring (diamine **B**) in **A**, the activity increased, providing 80% conversion at the same reaction time. It should be noted that the reaction is thermodynamically controlled. Nevertheless, when zeolite 4A was introduced to adsorb the water formed during the reaction with diamine **B**, the equilibrium was shifted, and 100% conversion with 100% selectivity was achieved after 3 h reaction time. The higher basicity of diamine **B** found in the catalytic test is likely due to the donating effect of methyl groups in position 3 of the cyclohexane ring. If this hypothesis were correct, then the presence of two additional methyl groups (diamine **C**) should give an even more active catalyst for the condensation reaction. However, contrary to the hypothesis, a lower catalytic activity was observed in this case (Fig. 1).

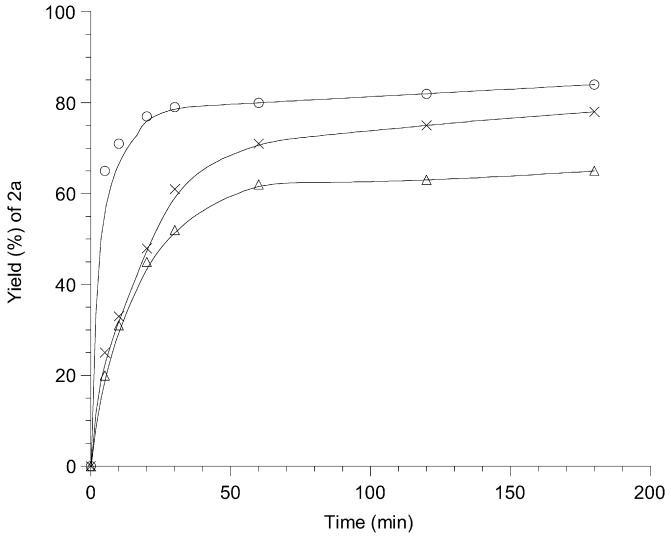


Fig. 1. Knoevenagel condensation of benzaldehyde (32 mmol) and ethyl cyanoacetate (28 mmol) without solvent at room temperature with diamine **A** (△) (0.14 mmol), diamine **B** (○), and diamine **C** (×).

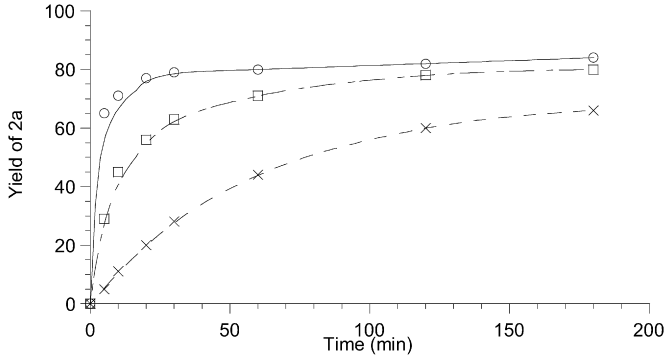


Fig. 2. Knoevenagel condensation of benzaldehyde (32 mmol) and ethyl cyanoacetate (28 mmol) without solvent at room temperature with diamine **B** (○), **DMAN** (□) and **TBD** (×) (0.14 mmol).

For comparison purposes, the condensation reaction was also performed in the presence of 1,5,7-triazabicyclo[4.4.0]dec-5-ene (TBD; Scheme 1) and the proton sponge **DMAN**. Results, shown in Fig. 2, demonstrate the following order of activity: **B** > **DMAN** > **TBD**. The fact that amine **B** exhibited higher activity than **DMAN** appears to indicate that the former behaved as a stronger base. The apparent activation energies ($E_{act}$) were estimated by performing the reaction at 273, 298, and 313 K and fitting the initial rate values to the Arrhenius equation, with a correlation coefficient of 0.99. The apparent $E_{act}$ for the reaction catalyzed by diamine **B** was

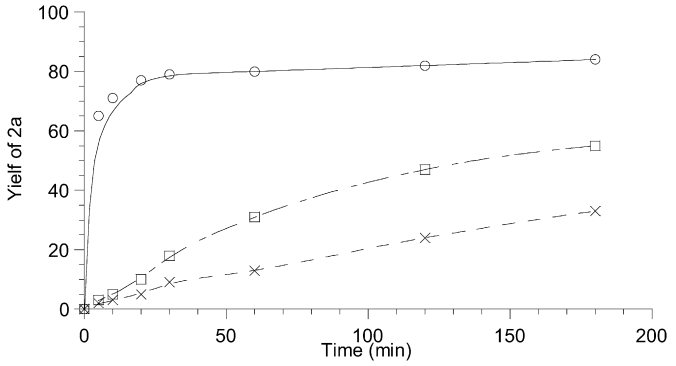


Fig. 3. Knoevenagel condensation of benzaldehyde (32 mmol) and ethyl cyanoacetate (28 mmol) without solvent at room temperature with diamine **B** (○), diamine **E** (□) and diamine **D** (×) (0.14 mmol).

$5 \pm 0.1$ kcal/mol, lower than that for **DMAN** (7.3 kcal/mol), consistent with the hypothesis of the stronger basicity of diamine **B**. In contrast, **TBD**, which has been claimed to be a strong basic catalyst able to perform various base-catalysed reactions, including carbonylation of amines [21], Michael-type additions [22] and transesterification reactions [23], exhibited much lower activity than diamine **B** and **DMAN**.

Because catalyst **B** has the greater catalytic activity, we explored another variable related to the molecular structure that may influence the basicity of **B**: increasing the distance between the two nitrogen atoms by means of two carbon bridges (diamine **E**; Scheme 1) instead of one carbon bridge between the two nitrogen atoms. Condensation of benzaldehyde with ethyl cyanoacetate (see Fig. 3) showed that the initial rate was lower for catalyst **E** than for catalyst **B**. In addition, the 3-methyl piperidine (**D**), which has only one amine group, is included for comparison. These results indicate that the molecular geometry of the catalyst plays an important role in catalytic activity, probably through the different stabilities of the reaction transition states.

Table 1 summarizes TOF values (initial reaction rate per mmol of catalyst) and yields at 1 h reaction time of 2a (see Scheme 2) obtained for the different amines evaluated. From the results presented, we can establish the following order of catalytic activity (initial rates) for the various catalysts tested: **B** > **DMAN** > **C** > **A** > **TBD** > **E** > **D**.

### 3.1. Theoretical calculations

To explain the catalytic results, we have considered that the proton affinity of the basic catalyst, as well as the geometry of the transition state (induced by the geometry of the basic molecule), can determine the energy of the proton transfer to and from the basic site. Indeed, it should be taken into account that although the proton may be easy to abstract from the reactant by the basic catalyst, the step of releasing the proton back to the catalyst may not be that easy or at least, when comparing different catalysts, may not maintain the correlation with proton affinity. If this is indeed the case, then the determinant property of a basic catalyst will necessarily be not the basic strength, but rather the kinetic activity, that is, adequate rates of proton transfer to and from the basic site [24]. It also has been reported that a usual drawback of, for instance, proton sponges, which are excellent from the standpoint of low nucleophilicity, can be the very low rates of proton transfer [9,25].

Table 1
Results of TOF and yield of 2a (see Scheme 2) obtained in the Knoevenagel condensation of benzaldehyde with ethyl cyanoacetate using different amines as base catalysts

| Catalysts (Scheme 1) | TOF ($min^{-1}$) | Yield of 2a[a] |
|---|---|---|
| **A** | 8.1 | 63 |
| **B** | 26.0 | 80 |
| **C** | 9.6 | 70 |
| **D** | 0.6 | 14 |
| **E** | 1.0 | 31 |
| **DMAN** | 11.2 | 71 |
| **TBD** | 2.2 | 45 |

[a] Benzaldehyde (32 mmol), ethyl cyanoacetate (28 mmol) catalyst (0.14 mmol) without solvent at room temperature at 1 h reaction time.

Table 2
Proton affinities (kcal/mol) calculated as differences in energy between neutral and protonated species. The quantum chemical calculations were performed by fully optimising the geometry of both species at the DFT/B3LYP 6-31G** level. Species are shown in Scheme 1

| Amines | Proton affinities (kcal/mol) |
|---|---|
| **DMAN** | 258.8 |
| Amine **E** | 258.2 |
| Amine **C** | 251.5 |
| Amine **B** | 250.9 |
| Amine **A** | 250.1 |
| Amine **D** | 241.8 |
| **TBD** (H1) | 232.2 |
| **TBD** (H2) | 233.3 |

In an attempt to correlate the catalytic activity with the basicity of the different catalysts, we calculated the proton affinities of the different amines as the energy difference between the neutral and the protonated forms of **DMAN** and amines **A**, **B**, **C**, **D**, and **E** (Scheme 1). The results, given in Table 2, show that **DMAN** was the most basic molecule, with a protonation energy of 258.8 kcal/mol, followed by (in order) the amines **E**, **C**, **B**, **A**, and **D**. The proton affinity of **TBD** also was calculated and found to be 232.2 or 233.3 kcal/mol, depending on whether the protonation occurs at N1 or N2 (Scheme 1). The order of the diamines **A**, **B**, and **C** indicates that the electron-donating methyl groups has an additive effect on increasing the electronic charge at the nitrogen atom, which can then stabilise the protonated form and increase the proton affinity. These amines contain two neighbour nitrogen atoms with relative orientation dictated by the rigidity of the piperidine cycle and the low flexibility of the $–CH_2–$ bridge between the two piperidine cycles. The optimisations show that in the protonated form, the lone pair of nitrogen cannot overlap with the proton as in **DMANH**$^+$ [9], resulting in poorer stabilisation of the protonated form and thus lower proton affinity with respect to **DMAN**. A different effect is seen in diamine **E**, in which the flexibility of the central $–CH_2–CH_2–$ group allows the correct reorientation of the two rings, enabling overlap of the nitrogen lone pair with the proton. The final geometry of the protonated form of diamine **E** gives a

bonding NH distance of 1.06 Å and a nonbonding N···H distance of 1.93 Å. In comparison, when the protonation of diamines **A** and **B** occurs, the bonding NH distance is 1.02 Å, whereas the nonbonding N···H distance is 2.52 Å. This indicates a lower proton affinity and a greater ability to release the proton back in diamines **A** and **B** with respect to diamine **E**.

Up to now, we have shown that the proton affinities calculated for **TBD** and diamines **D**, **A**, and **B** correlate with the catalytic activity observed, with amine **B** (which exhibits the higher proton affinity) exhibiting the greatest catalytic activity. However, there are exceptions to the direct correlation between proton affinity and catalytic activity. In our case, we have seen that amines **C**, **E**, and **DMAN**, despite their higher proton affinity compared with amine **B**, exhibit lower catalytic activity. For amine **C**, the lower activity with respect to **B** can be attributed to the presence of the four methyl groups in the piperidine rings, which can cause steric hindrance of proton abstraction. However, for amines **E** and **DMAN**, the lower catalytic activity exhibited with respect to the amine **B** may be related to a lower rate of proton transfer from the basic site to the oxoanion intermediate, although another possibility, involving the difficulty of protonating the base due to steric problems, also may explain the catalytic results. To clarify this point, following the reaction mechanisms presented in Scheme 4, we studied the different reaction steps by means of computational chemistry techniques.

### 3.2. Knoevenagel condensation using amine *B*

The first step (step 1 in reaction (1) of Scheme 4) is protonation of amine **B**, in which the hydrogen of the methylene group is transferred to the amine [12]. This is shown in Fig. 4, which characterises the reactant, product, and transition state. An activation energy of 8.8 kcal/mol has been found for this reaction.

The second step (step 2 in reaction (1) of Scheme 4) proceeds by approaching the benzaldehyde to the resulting ethyl cyanoacetate anion to form an adduct with a negative charge localised in the carbonyl oxygen of benzaldehyde, which becomes simply bonded to the carbon atom. This reaction, in which all of the species involved have been characterised, is shown in Fig. 4; an activation energy of 8.4 kcal/mol has been calculated.

*The third step* (step 3 in reaction (1) of Scheme 4) of the reaction [12] occurs between the adduct and the basic catalyst (amine **B**), which, by giving back the proton, forms the final Knoevenagel condensation product. The proton is given back very easily because the reaction proceeds without activation energy, as can be seen from the species characterised in Fig. 4.

We have not considered the final elimination step, because the dehydration of the alcohol intermediate giving the cinnamate is very rapid, and it is rarely found to be the controlling step [26].

### 3.3. Knoevenagel condensation using *DMAN*

The *first step* (step 1 in reaction (2) of Scheme 4) is the protonation of **DMAN**. Fig. 5 shows the characterisation of the reactant, product, and transition state. The activation energy is 22.4 kcal/mol for this reaction; this high value is due to the fact that the incoming acid molecule, when approaching the proton-attracting (N···N) location in the **DMAN** molecule, finds a steric hindrance due to the bulky methyl groups, precluding an otherwise easy approach between the acid and basic molecules. Further along in the reaction, this forces a nonoptimised angular behaviour of the lone pairs of the N atoms in the **DMAN** molecule that, together with the problems in the further approach of the acid molecule, yields a transition state of high energy. Despite the clear proton-attracting power of the **DMAN** molecule, as reflected in its high proton affinity (Table 2), the overall result of the reaction analysis indicates a series of problems resulting in a high activation energy. An analysis of the calculated geometries shown in Fig. 5 indicates the following relevant bond distances in the transition state geometry: $r(\mathrm{NH}) = 1.222$ Å and $r(\mathrm{CH}) = 1.562$ Å. In the equivalent transition state of the same reaction with amine **B** (Fig. 4), we have $r(\mathrm{NH}) = 1.214$ Å and $r(\mathrm{CH}) = 1.510$ Å, indicating that the proton in the transition state is less transferred to the amine (and less detached from the ethyl cyanoacetate) when using **DMAN**, at a higher activation energy (22.4 kcal/mol, compared with 8.8 kcal/mol in Table 3).

The *second step* (step 2 in reaction (2) of Scheme 4) proceeds exactly the same as with the previous catalyst, because this is a condensation reaction between benzaldehyde and ethyl cyanoacetate anion that forms an adduct, with the catalyst playing no role whatsoever. Therefore, the species involved, as shown in Fig. 5, are the same as in step 2 of reaction (1), and the same activation energy of 8.4 kcal/mol holds for this case as well. Although initially the counterion may play a role in this reaction, this is considered negligible, because the anionic complex between the carbanion and the benzaldehyde is so bulky that the counterion is at a considerable separation. Also, taking into account that the counterion (the corresponding protonated amine, either amine **B** or **DMAN**) is itself also a bulky molecule adds to the considerable separation between the cation and the anion, which all together results in a less important ionic interaction with the cation and thus a negligible role of the cation in step 2 of the reaction.

Table 3
Energies of the molecular species corresponding to the reaction between ethyl cyanoacetate, amine **B**, and benzaldehyde (reaction (1) in Scheme 4); and to the reaction between ethyl cyanoacetate, **DMAN**, and benzaldehyde (reaction (2) in Scheme 4). The energies were obtained by ab initio Hartree–Fock calculations with 3-21G basis set. Details of the geometries are shown in Figs. 4 and 5. The energies of the reactants, transition states and products are in units of Hartrees (1 Hartree/particle is 627.50959 kcal/mol)

| | Reactant | Transition state | Product | $E_{act}$[b] |
|---|---|---|---|---|
| Step 1 (amine **B**) | −1008.29629 | −1008.28233 | −1008.28426 | 8.8 |
| Step 2[a] | −736.32293 | −736.30956 | −736.31457 | 8.4 |
| Step 3 (amine **B**) | −1349.82254 | – | −1349.84594 | – |
| Step 1 (**DMAN**) | −1041.26760 | −1041.23186 | −1041.24206 | 22.4 |
| Step 3 (**DMAN**) | −1382.78056 | −1382.77410 | −1382.81084 | 4.1 |

[a] Step 2 is the same regardless the base used (either amine **B** or **DMAN**), as can be seen from Scheme 4.
[b] Activation energies ($E_{act}$) are in kcal/mol.

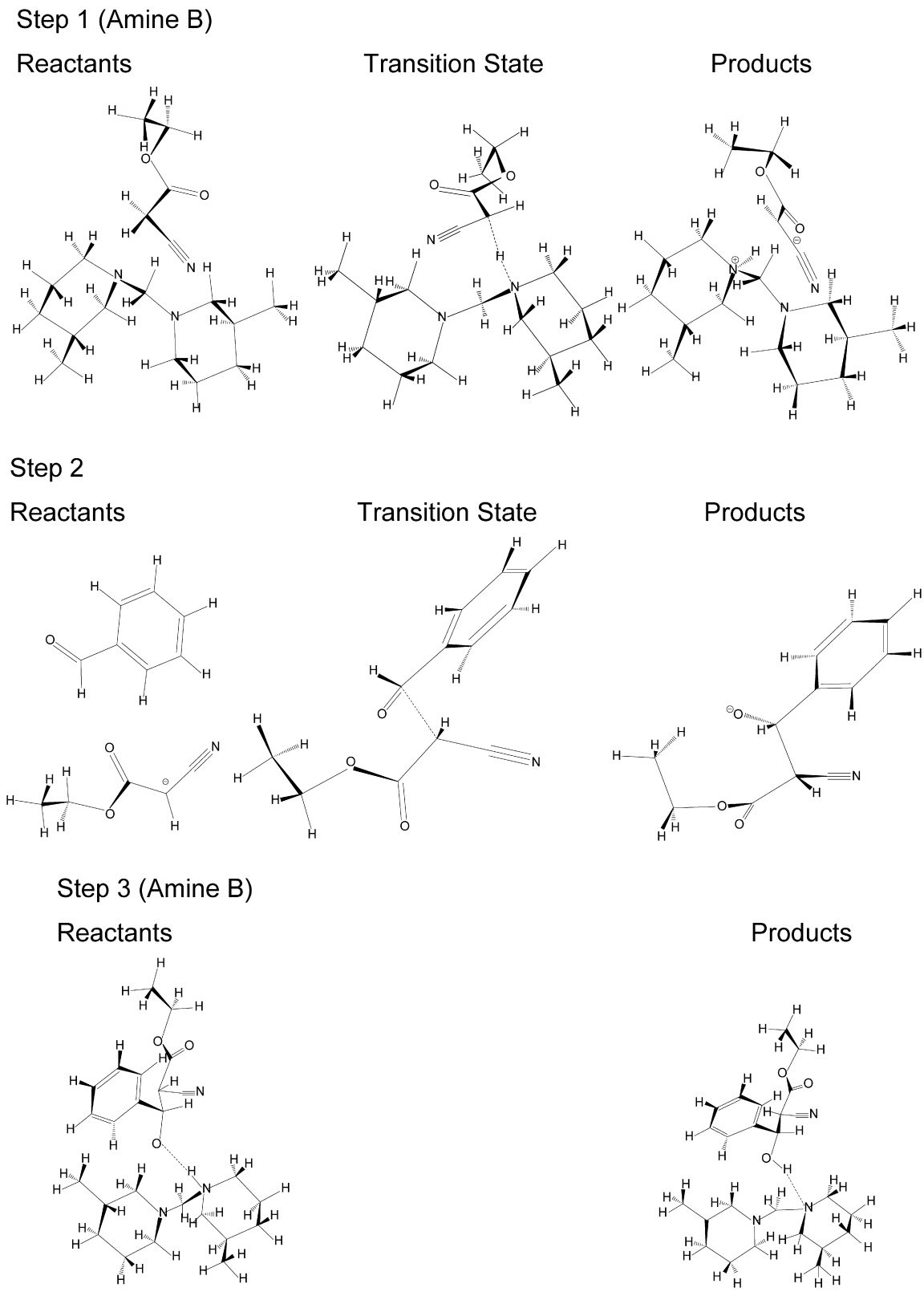


Fig. 4. Molecular species corresponding to the reaction between ethyl cyanoacetate, amine **B**, and benzaldehyde (this corresponds to reaction (1) in Scheme 4). The drawings correspond to the geometries obtained by ab initio Hartree–Fock calculations with 3-21G basis set, and the corresponding energies are in Table 3. The relevant bond distances for step 1 are: (a) reactants: $r$(NH) = 1.848 Å, $r$(CH) = 1.127 Å; (b) transition state: $r$(NH) = 1.214 Å, $r$(CH) = 1.510 Å; (c) products: $r$(NH) = 1.002, $r$(CH) = 1.954 Å. The relevant bond distances for step 2 are: (a) reactants: $r$(CO) = 1.219 Å; (b) transition state: $r$(CC) = 1.979 Å, $r$(CO) = 1.274 Å; (c) products: $r$(CC) = 1.627, $r$(CO) = 1.352 Å. The relevant bond distances for step 3 are: (a) reactants: $r$(NH) = 1.008 Å, $r$(OH) = 1.465 Å; (b) products: $r$(NH) = 1.709, $r$(OH) = 1.002 Å.

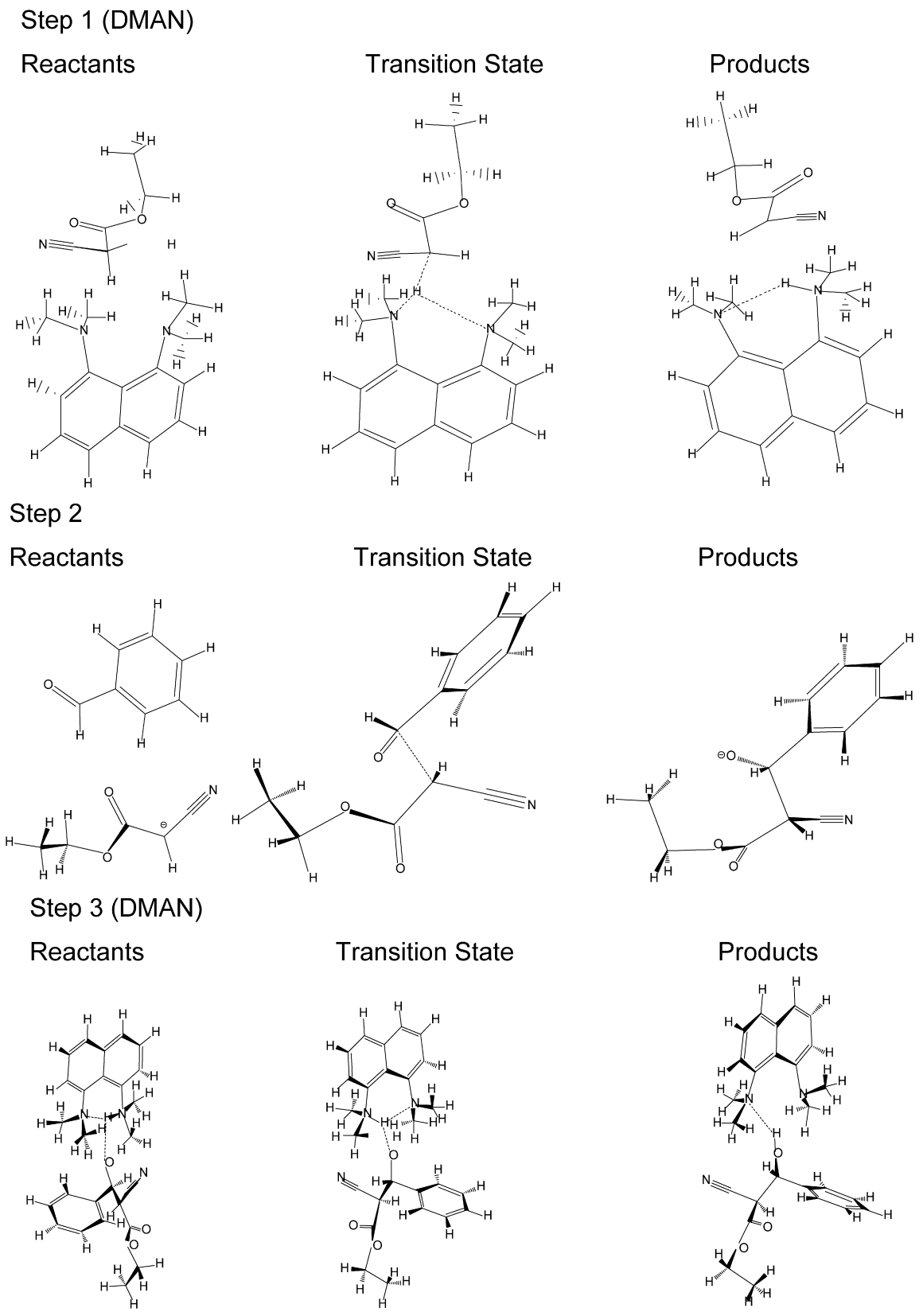


Fig. 5. Molecular species corresponding to the reaction between ethyl cyanoacetate, DMAN, and benzaldehyde (this corresponds to reaction (2) in Scheme 4). The drawings correspond to the geometries obtained by ab initio Hartree–Fock calculations with 3-21G basis set, and the corresponding energies are in Table 3. The relevant bond distances for step 1 are: (a) reactants: $r$(NH) = 2.557 Å, $r$(CH) = 1.090 Å; (b) transition state: $r$(NH) = 1.222 Å, $r$(CH) = 1.562 Å; (c) products: $r$(NH) = 1.032 Å, $r$(CH) = 2.464 Å. The relevant bond distances for step 2 are: (a) reactants: $r$(CO) = 1.219 Å; (b) transition state: $r$(CC) = 1.979 Å, $r$(CO) = 1.274 Å; (c) products: $r$(CC) = 1.627, $r$(CO) = 1.352 Å. The relevant bond distances for step 3 are: (a) reactants: $r$(NH) = 1.069 Å, $r$(OH) = 2.491 Å; (b) transition state: $r$(NH) = 1.054 Å, $r$(OH) = 1.806 Å; (c) products: $r$(NH) = 2.155, $r$(OH) = 0.979 Å.

The *third step* (step 3 in reaction (2) of Scheme 4) of the reaction occurs between the adduct and the protonated **DMAN**, which, by giving back the proton, forms the final Knoevenagel condensation product. Instead of a reaction without activation energy (as occurs in step 2 of reaction (1)), this reaction gives an activation energy of 4.1 kcal/mol, as shown for the species characterised in Fig. 5 and Table 3. Again, the approach between the reactants is hindered by the bulky oxoanion and its interaction with the methyl groups of the **DMANH**$^+$ molecule. This results in an activation energy higher than that of the corresponding step 3 of the previous reaction (reaction (1) with amine **B**).

### 3.4. Comparison between the results of the Knoevenagel condensation using amine *B* and *DMAN*

After rationalising why the activation energies (shown in Table 3) are higher or lower in each case, a simple analysis of the overall results shows that in either case (reaction (1) or reaction (2)), the rate-determining step is step 1. This points to the fact that the capability to accept the proton is controlling the overall reaction rate, and this is easier when amine **B** instead of **DMAN** is used as catalyst, despite the fact that **DMAN** has a higher proton affinity than amine **B**. Consequently, from our reaction study, we have established a difference between the ideal capacity of accepting protons (proton affinity, as shown in Table 2) and the actual capacity of accepting protons, which depends on other factors besides proton affinity, which in this case are dominated by steric hindrance, as explained in the previous paragraphs.

The above calculations also indicate that basicity is not the only characteristic that can explain the relative order of catalytic activity when using different catalysts. Along with the ability to stabilise the proton (proton affinity; step 1), proton release (step 3) also must be considered. The steric conformation between amine **B** and the negatively charged adduct (see Fig. 4) allows proton elongation from amine **B** and its transfer to the oxoanion without activation energy much more easily than can occur in **DMAN**, in which the proton is more firmly attached and the release requires activation energy (4.1 kcal/mol). Although the protonic transfer to an anion should be considered an easy reaction with no activation energy, geometry and initial conformations (Fig. 5) show that the proton is shielded and protected in the **DMANH**$^+$ cation, and thus the strong tendency to transfer this to a negatively charged molecule does not occur until the proton is separated from its initial geometry, which requires an activation energy. Although step 3 is not the controlling step in this case, nevertheless it also should be considered.

These results explain the experimental observations in the sense that the most basic **DMAN** catalyst does not give the largest conversion, which is found for amine **B**. Recall that this is explained by the higher activation energy of step 1 when using **DMAN** compared with using amine **B**, with the latter giving a lower activation energy and thus greater conversion, as shown from the experimental results in Fig. 2.

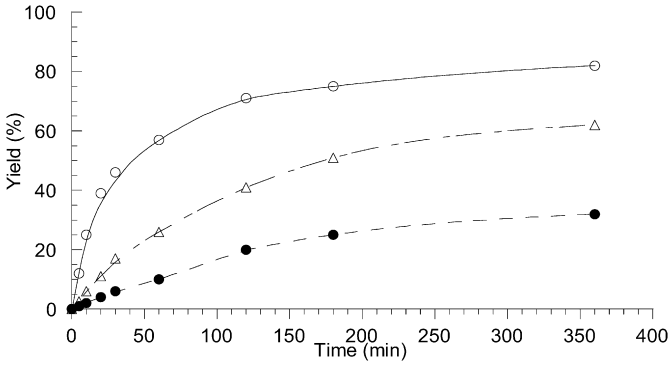


Fig. 6. Condensation of benzaldehyde (32 mmol) with: (○) ethyl acetoacetate (28 mmol), amine **B** (0.14 mmol) at 60 °C; (△) diethyl malonate (28 mmol), amine **B** (0.28 mmol) at 80 °C; (●) acetophenone (28 mmol), amine **B** (0.28 mmol) at 130 °C.

### 3.5. Carbon–carbon bond formation with different reactants

To estimate the capacity of amine **B** for abstracting protons with p$K_a > 9$, we performed Knoevenagel condensation of benzaldehyde with more demanding basic strength methylenic active compounds, ethyl acetoacetate (p$K_a = 10.9$) and diethyl malonate (p$K_a = 13.3$). Moreover, we tested the Claisen–Schmidt condensation between acetophenone (p$K_a = 15.8$) and benzaldehyde. Fig. 6 shows the results obtained for the three substrates. In all cases, the selectivities for the condensation products are 100%. Fig. 6 shows that the order of activity correlates with the p$K_a$ of the different acidic substrates: **1a** > **1b** > **1c** > acetophenone. On the other hand, we have previously found [9] that when carrying out the condensation of ethyl acetoacetate with benzaldehyde in the presence of **DMAN** and the absence of solvent, no condensation occurred. This behaviour was attributed to the fact that the protonated **DMAN** is so stable that the proton is not returned toward the oxoanion intermediate, and thus the catalyst becomes inactive. However, when the condensation is carried out in the presence of a solvent such as DMSO, which polarizes the N–H$^+$–N bond, the intramolecular hydrogen bond of the protonated **DMAN** loses strength, facilitating release of the proton, after which the catalyst becomes active. We conclude that diamine **B** has a strong basic character, with the ability to abstract protons with p$K_a$ up to 15.8 (see Fig. 6). This can be attributed to the combination of two factors: the high proton affinity and the ability to return the proton to the oxoanion intermediate.

### 3.6. Influence of the solvent on catalytic activity

It is known that when charged species are involved in a reaction, changes in the polarity of the media can strongly affect the reaction rate. We investigated the influence of the solvent on the rate of reaction between benzaldehyde and ethyl acetoacetate, using amine **B** as the catalyst in the presence of solvents with different dielectric constants, $\varepsilon$: DMSO ($\varepsilon = 48.9$), DMF ($\varepsilon = 36.7$), EtOH ($\varepsilon = 24.3$), *t*-butanol ($\varepsilon = 12.47$), chlorobenzene ($\varepsilon = 5.6$), and toluene ($\varepsilon = 2.4$). Fig. 7 shows the yields of the Knoevenagel adduct versus reaction time. As can be

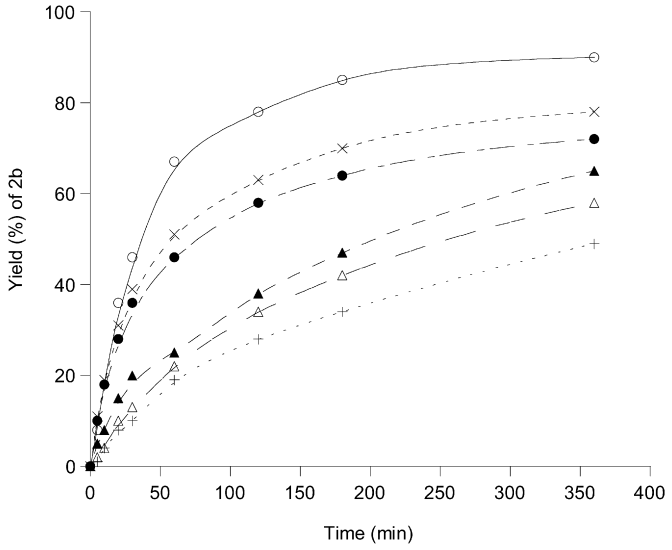


Fig. 7. Condensation of benzaldehyde (32 mmol) and ethyl acetoacetate (28 mmol) at 60 °C with diamine **B** (0.14 mmol) in different solvents (5 mL): DMSO (○); DMF (×); EtOH (●); *t*-butanol (▲); chlorobenzene (△); toluene (+).

seen, the greatest activity is obtained with the most polar solvents [9], (see also the relative rates of ethanol and *tert*-butanol in Fig. 7), and the order of reactivity correlates very well with the dielectric constant: DMSO > DMF > EtOH > *t*-butanol > chlorobenzene > toluene. Furthermore, when the condensation reaction is carried out with nonpolar solvents, the reaction rate decreases significantly, as occurs when the reaction involves a charged transition state or a neutral but polarizable transition state formed through a single concerted step.

## 4. Conclusion

In this work, diamines with neighbour nitrogen atoms were used as base catalysts in the Knoevenagel condensation reaction between benzaldehyde and ethyl cyanoacetoacetate. The diamines used as catalysts show the feature of stabilising the proton abstracted in the first step of the reaction due to the effect of a N–$H^+$–N interaction between the neighboring atoms of the diamine. Nevertheless, the catalytic results do not show a correlation between proton affinity of the diamine and basic strength, suggesting that other effects related to the mechanism should be studied. Computational chemistry techniques have been used to study the three steps of the Knoevenagel condensation using amine **A** and **DMAN** as catalysts and the results show that the rate-determining step is step 1, which involves release of the proton to the basic catalyst. The ability to accept the proton by the basic molecules does not correlate with the calculated proton affinities due to the influence of steric factors, making it more difficult to accept the proton when the catalyst is **DMAN**. Therefore, the reaction rate is higher when using amine **B**, which explains the greater conversions found experimentally when using amine **B** compared with **DMAN**.

## Acknowledgments

Support was provided by the Ministerio de Educacion y Cultura of Spain (project MAT2003-07769-C02-01) and the Generalidad Valenciana (GV04B-270). I.D. thanks the Consejo Superior de Investigaciones Científicas for an I3P fellowship. G.S. thanks Centro de Investigaciones Energeticas, Medioambientales y Tecnologicas and Centro de Proceso de Datos, Universidad Politecnica de Valencia for the use of their computational facilities. The contribution of Mr. Pablo Ramos to the experimental work reported herein is also gratefully acknowledged.

## References

[1] M.J. Climent, A. Corma, S. Iborra, A. Velty, J. Catal. 221 (2004) 472.
[2] A. Cauvel, G. Renard, D. Brunel, J. Org. Chem. 62 (1997) 749.
[3] (a) M. Laspéras, T. Llorett, L. Chaves, I. Rodriguez, A. Cauvel, D. Brunel, Stud. Surf. Sci. Catal. 108 (1997) 75;
(b) F. Bigi, S. Carloni, R. Maggi, A. Mazzacani, G. Sartori, Stud. Surf. Sci. Catal. 130 (2000) 3501;
(c) I. Rodriguez, S. Iborra, A. Corma, Appl. Catal. 194–195 (2000) 241.
[4] (a) Y.V. Subba Rao, D.E. De Vos, P.A. Jacobs, Angew. Chem. Int. Ed. Engl. 36 (1997) 2661;
(b) R. Sercheli, R.M. Vargas, R. Sheldon, U. Schuchardt, J. Mol. Catal. A 148 (1999) 173;
(c) S. Jaenicke, G.K. Chuah, X.H. Lin, X.C. Hu, Microporous Mesoporous Mater. 35–36 (2000) 143;
(d) A.C. Blanc, D.J. Macquarrie, S. Valle, G. Renard, C.R. Quinn, D. Brunel, Green Chem. 2 (2000) 383.
[5] A. Corma, S. Iborra, I. Rodriguez, F. Sanchez, J. Catal. 211 (2002) 208.
[6] J.-P. Besse, D. Brunel, P. Massiani, D. Tichit, Actual. Chimique 5–6 (2002) 111.
[7] R.W. Alder, Chem. Rev. 89 (1989) 1215.
[8] (a) H.A. Staab, T. Saupe, Angew. Chem Int. Ed. Engl. 27 (1988) 865;
(b) A.L. Llamas-Saiz, C. Foces-Foces, J. Elguero, J. Mol. Struct. 328 (1994) 297.
[9] I. Rodriguez, G. Sastre, A. Corma, S. Iborra, J. Catal. 183 (1999) 14.
[10] (a) B. Siebenhaar, WO 9721659 (1997);
(b) A.J. Kesel, W. Oberthür, WO 9820013 (1998);
(c) J.P. Ferraris, T.L. Lambert, S. Rodriguez, WO 9305077 (1993).
[11] (a) A. Corma, V. Fornes, R.M. Martin-Aranda, F. Rey, J. Catal. 134 (1992) 58;
(b) M.J. Climent, A. Corma, V. Fornés, A. Frau, R. Guil-Lopez, S. Iborra, J. Primo, J. Catal. 163 (1996) 392.
[12] (a) F.S. Prout, U.D. Beaucaire, G.R. Dyrkarcz, W.M. Koppes, R.E. Kuznicki, T.A. Marlewski, J.A. Pienkowski, J.M. Puda, J. Org. Chem. 38 (1973) 1512;
(b) G. Jones, Org. React. 15 (1967) 204;
(c) J. Guyot, A. Kergomard, Tetrahedron 39 (1983) 1166.
[13] V.K. Valerij, G.I. Rutman, USSR SU1482910 (1989).
[14] (a) J.S. Binkley, J.A. Pople, W.J. Hehre, J. Am. Chem. Soc. 102 (1980) 939;
(b) M.S. Gordon, J.S. Binkley, J.A. Pople, W.J. Pietro, W.J. Hehre, J. Am. Chem. Soc. 104 (1982) 2797;
(c) W.J. Pietro, M.M. Francl, W.J. Hehre, D.J. Defrees, J.A. Pople, J.S. Binkley, J. Am. Chem. Soc. 104 (1982) 5039.
[15] H.B. Schlegel, J. Comput. Chem. 3 (1982) 214.
[16] (a) J. Simons, P. Jorgensen, H. Taylor, J. Ozment, J. Phys. Chem. 87 (1983) 2745;
(b) A. Bannerjee, N. Adams, J. Simons, R. Shepard, J. Phys. Chem. 89 (1985) 52.
[17] (a) J.T. Golab, D.L. Yeager, P. Jorgensen, Chem. Phys. 78 (1983) 175;
(b) C.J. Cerjan, W.H. Miller, J. Chem. Phys. 75 (1981) 2800.
[18] A.D. Becke, J. Chem. Phys. 10 (1993) 5648.
[19] (a) R. Ditchfield, W.J. Hehre, J.A. Pople, J. Chem. Phys. 54 (1971) 724;
(b) W.J. Hehre, R. Ditchfield, J.A. Pople, J. Chem. Phys. 56 (1972) 2257;

(c) P.C. Hariharan, J.A. Pople, Mol. Phys. 27 (1974) 209;
(d) M.S. Gordon, Chem. Phys. Lett. 76 (1980) 163;
(e) P.C. Hariharan, J.A. Pople, Theor. Chim. Acta 28 (1973) 213.

[20] M.J. Frisch, G.W. Trucks, H.B. Schlegel, G.E. Scuseria, M.A. Robb, J.R. Cheeseman, V.G. Zakrzewski, J.A. Montgomery Jr., R.E. Stratmann, J.C. Buran, S. Dapprich, J.M. Millam, A.D. Daniels, K.N. Kudin, M.C. Strain, O. Farkas, J. Tomasi, V. Barone, M. Cossi, R. Cammi, B. Mennucci, C. Pomelli, C. Adamo, S. Clifford, J. Ochterski, G.A. Petersson, P.Y. Ayala, Q. Cui, K. Morokuma, N. Rega, P. Salvador, J.J. Dannenberg, K.D. Malick, A.D. Rabuck, K. Raghavachari, J.B. Foresman, J. Cioslowski, J.V. Ortiz, A.G. Baboul, B.B. Stefanov, G. Liu, A. Liashenko, P. Piskorz, I. Komaromi, R. Gomperts, R.L. Martin, D.J. Fox, T. Keith, M.A. Al-Laham, C.Y. Peng, A. Nanayakkara, M. Challacombe, P.M.W. Gill, B. Johnson, W. Chen, M.W. Wong, J.L. Andres, C. Gonzalez, M. Head-Gordon, E.S. Replogle, J.A. Pople, Gaussian 98, Revision A.11.2, Gaussian, Inc., Pittsburgh, PA, 1998.

[21] R. Ballini, D. Fiorini, R. Maggi, P. Righi, G. Sartori, R. Sartorio, Green Chem. 5 (2003) 396.

[22] (a) E. Van Aken, H. Wynberg, F. Van Bolhuis, Acta Chem. Scand. 47 (1993) 122;
(b) D. Bensa, J. Rodriguez, Synth. Commun. 34 (2004) 1515;
(c) A. Horvath, Tetrahedron Lett. 37 (1996) 4423.

[23] (a) F. Jerome, G. Kharchafi, I. Adam, J. Barrault, Green Chem. 6 (2004) 7;
(b) A.L.M. Guimaraes, R.M. Vargas, J. Am. Oil Chem. Soc. 75 (1998) 755;
(c) U. Schuchardt, R.M. Vargas, G. Gelbard, J. Mol. Catal. A 99 (1995) 65.

[24] R.W. Alder, J. Am. Chem. Soc. 127 (21) (2005) 7924.

[25] (a) R.W. Alder, N.C. Goode, N. Miller, F. Hibbert, K.P.P. Hunte, H.J. Robbins, J. Chem. Soc. Chem. Commun. (1978) 89;
(b) F. Hibbert, G.R. Simpson, J. Chem. Soc. Perkin Trans. 2 (1987) 243.

[26] (a) S. Patai, Y. Israeli, J. Chem. Soc. (1960) 2025;
(b) R.L. Reeves, S. Patai (Eds.), The Chemistry of Carbonyl Group, Interscience, New York, 1966, p. 567.